Collisional Evolution of the Main Asteroid Belt

William Bottke
Southwest Research Institute and the Institute for the Science of Exploration Targets (ISET), 1050 Walnut St, Suite 300, Boulder, CO

Miroslav **Mira Brož**
FILL THIS IN

David P. O'Brien
Planetary Science Institute, 1700 E. Ft. Lowell, Suite 106, Tucson, AZ

Adriano Campo-Bagatin
FILL THIS IN

Alessandro Morbidelli
FILL THIS IN

Simone Marchi
Southwest Research Institute and the Institute for the Science of Exploration Targets (ISET), 1050 Walnut St, Suite 300, Boulder, CO

Collisional evolution models have provided us with many insights planetesimal and planet formation scenarios as well as how the main belt reached its current state. By implementing what has been learned about asteroid collisional and dynamical evolution aeross a wide range of disciplines, these models predict that the asteroid belt experienced as much comminution over its early history as it has since it reached its low-mass state approximately 4 Ga. This makes the main belt's wavy size-frequency distribution a "fossil" of a violent early epoch. In addition, these same models predict that most $D > 100$ km diameter and larger asteroids are probably primordial, with their physical properties mainly determined during the accretion epoch. The main belt size distribution evolves to a collisional steady state, where it keeps the same approximate shape for most of its lifetime. This attribute can be used to explain why the non-saturated crater size frequency distributions found on main belt asteroids have similar shapes. The near-Earth asteroid size distribution can also be considered a reflection of this population, with a relatively constant flux of asteroids striking the terrestrial planets for billions of years.

1. INTRODUCTION

The main asteroid belt is a living relic. It contains a record of what happened to much of the Solar System since the planet formation epoch. Ongoing collisional and dynamical evolution processes, however, are slowly obscuring the traces left behind. The goal of modeling efforts is to use all possible data to discern the initial conditions and evolution processes that occurred during and after the planet formation epoch. For example, the questions one can probe with main belt constraints include using the asteroid belt to tell us about nature and mass of planetesimals inside of Jupiter's orbit, the timing of Jupiter's formation, the distribution of volatiles in the inner solar system, the size distribution produced during planetary accretion, the scaling laws that control collisional evolution both during and after planetary accretion, the presence of planetary embryos inside Jupiter's orbit, the migration of the giant planets and whether sweeping resonance ever crossed the main belt, the degree of material mixing that occurred between the feeding zones, etc.

A major uncertainty in any collisional evolution model of the asteroid belt concerns what happened when planet formation processes and/or giant planet migration was taking place. Many scenarios have been investigated over the last several decades, with the latest thinking discussed in the chapter by Morbidelli et al. In essence, the various scenarios can be distilled down into a few broad themes. ...

The total mass of the main asteroid belt, which is dominated by the masses of the largest asteroids, is $\sim 6 \times 10^{-4}$ Earth masses **or** 3.6×10^{24} **g**. This mass is very small compared to the mass of solids that were thought to exist in the main belt region at the time of asteroid formation. For example, the *minimum mass solar nebula* (MMSN; Weidenschilling, 1977; Hayashi, 1981) suggests that 1-2.5 Earth masses of solid material once existed between 2 and 3 AU.

This implies the main belt region could be deficient in mass by a factor 1,500-4,000, provided planetesimal formation was an efficient process (see chapter by Johansen et al.). Taken at face value, these values are often used to argue that the asteroid belt has lost more than 99.9% of its primordial mass. If true, the current mass deficit in the main belt larger than a factor of 1,000.

If so much mass once existed in the primordial main belt region, collisional evolution, dynamical removal processes, or some combination of the two were needed to get rid of it and ultimately produce the current main belt population. Many attempts have been made to reproduce the mass deficit by collisions alone; see Davis et al. (2002) for a ~~recent~~ review. The problem with doing so is twofold. First, it is difficult for collisions alone to grind away the main belt size distribution predicted by accretion models without eliminating Vesta's crust or producing size distributions that are highly inconsistent with the observed main belt size distribution (e.g., Davis et al. 1985). Second, collisional ~~evolution results generated~~ using disruption scaling laws based on numerical hydrocode simulations of asteroid collisions (e.g., Benz and Asphaug 1999) cannot break up sufficient $D > 100$ km asteroids to reproduce the observed population.

Taken together, these outcomes suggest that either dynamical removal of asteroids has played a strong role in allowing the population to reach its current state (see chapter by Morbidelli et al.), or that the main belt size distribution for the largest asteroids has not changed very much since planetesimal formation. For the former, several scenarios have been suggested to remove most of the primordial main belt's mass. For example, planetary embryos may have initially formed in the main belt region. As they gravitationally excited themselves and the surrounding planetesimals, most of these bodies would escape, thereby naturally creating much of the main belt mass deficit. In a second and somewhat related scenario, Jupiter gravitationally interacts with the gas disk and migrates across the main belt region. This so-called Grand Tack scenario allows Jupiter to do the job of scattering embryos and planetesimals out of the main belt region. The key similarity in both scenarios is planetesimals that were dynamical excited out of the main belt have the opportunity to slam into the survivors left behind. This allows these models to be at least partially tested against collisional constraints.

An alternative scenario is to assume that planetesimal and planet formation works differently than has been assumed to date, and that the quantity of planetesimals in the main belt region was never more than a few times the present-day population (e.g., Levison et al. 2014a,b). This would remove the need for a mass deficit. This new scenario would invoke a new process called "pebble accretion", where planetesimal growth rates are strongly linked to how small bodies interact with the gas of the solar nebula (e.g., see chapter by Johansen et al.). If viable, the degree of collisional evolution would be dominated not by the material lost from the primordial main belt, but rather by impacts from leftover planetesimal populations found outside the main belt region.

Beyond the earliest times, there is also the issue of how the main belt region was affected by late giant planet migration, or what is often referred to as the Nice model (see chapter by Morbidelli et al.). In these scenarios, the main belt spent hundreds of My with a population that was only a few times larger than its current mass. It may also have had a stable extension between 1.8-2.1 AU (called the E-belt) that was also filled with a comparable number density of asteroids (Bottke et al. 2012). When a dynamical instability took place in the outer solar system, the gas giants migrated to their current locations and secular resonances swept across the main belt region. This would have caused the main belt to lose several times its current mass and the E-belt. Interestingly, resonance sweeping cannot remove much of the main belt's population without producing observable dynamical damage [REF], which means it cannot be a major player in explaining the main belt's mass deficit.

The question is how to test these concepts with what we know about asteroids and the asteroid belt itself, and whether asteroid belt constraints are sufficient at this time to eliminate various planet formation and evolution scenarios. To do this, we first examine the processes affecting asteroidal collisional evolution, and what would need to be incorporated into a comprehensive collisional evolution model (Sec. 2). Next, we need to discuss the constraints that can be reasonably brought to bear on this problem (Sec. 3). Only then can we discuss what we have learned from existing models (Sec. 4).

In science, it is often more interesting to rule out particular scenarios, and generate new constraints in the process, than to find yet another non-unique solution that may fit the data. One of the key attributes of studying the collisional evolution of the main belt, therefore, is to see what evolution scenarios do not fit. Then, as new data comes in, we are prepared to glean new insights into planet and planetesimal formation processes with our increasingly sophisticated and realistic models.

2. Processes Affecting Main Belt Evolution

Most collision evolution models involve the solution of a straightforward differential equation, though the details can be quite complicated and somewhat messy from an accounting standpoint. The starting point is an initial size-frequency distribution (SFD) for the asteroid belt, where the bodies in the population (N) has been binned in logarithmic intervals as a function of diameter. The goal is then to compute the time rate of change in the population per unit volume of space over a size range between diameter D and $D+dD$ (Dohnanyi 1969; Williams and Wetherill 1994). In a schematic form, it can be written as:

$$\frac{\partial N}{\partial t}(D,t) = -I_{\rm COLL} + I_{\rm FRAG} - I_{\rm DYN}. \qquad (1)$$

Here $I_{\rm COLL}$ is the net number of bodies that leave between D and $D + dD$ per unit time from cratering or catastrophic disruption event. This value is calculated at every timestep by determining how many projectiles from other size bins are capable of producing either a cratering event (of interest) or a catastrophic disruption event among bodies between D and $D + dD$. Thus, this function is a "sink" for bodies in the SFD.

The results of this calculation are sent to the function $I_{\rm FRAG}$, which is the number of bodies entering a given size bin per unit time that were produced via the fragmentation of larger bodies. This function tells about the "source" of new material, with big bodies acting as a reservoir that can create new smaller bodies.

Finally, the equation accounts for $I_{\rm DYN}$, which is the number of bodies lost from a given size bin via dynamical processes, such as an object escaping through a dynamical resonance. This function is a sink for bodies in the SFD.

In the sections below, we discuss the many parameters and mechanisms needed to understand and create these functions within a collision evolution code. We also discuss the possibility of including additional functions, such as allowing non-gravitational forces like YORP spin-up torques to act as an additional sink for small bodies (see chapter by Vokrouhlický et al.).

2.1 Asteroid Collision Probabilities

A necessary component to determining the collisional evolution of a population is to compute the impact probabilities and velocities between individual bodies. They are used to estimate the interval between cratering and catastrophic disruption events for target bodies of different sizes. The most common value used in these cases is the intrinsic collision probability P_i, defined as the likelihood that a single member of the impacting population will hit the target over a unit of time, and the mean impact velocity $V_{\rm imp}$ between the bodies in question (e.g., Öpik 1951; Wetherill 1967; Greenberg 1982; Farinella and Davis 1992; Bottke and Greenberg 1993).

To get these values for the present-day main belt, Bottke et al. (1994) took a representative sample of main-belt asteroids (e.g., 682 asteroids with $D > 50$ km as defined by Farinellla and Davis 1992) and calculated P_i and $V_{\rm imp}$ between all possible pairs of asteroids, assuming fixed values of semimajor axis, eccentricity, and inclination (a, e, i). A common approximation made here is that the orbits can be integrated over uniform distributions of longitudes of apsides and nodes because secular precession randomizes their orbit orientations over $\sim 10^4$ year timescales. After all possible orbital intersection positions for each projectile-target pair were evaluated and weighted, they found that main belt objects striking one another have $P_i \sim 2.86 \times 10^{-18}$ km^{-2} yr^{-1} and $V_{\rm imp} \sim 5.3$ km s^{-1}. These values have been corroborated by several different groups and methods (e.g., Farinella and Davis 1992; Vedder 1998; dell'Oro and Paolicchi 1998; Manley et al. 1998).

To model collisional evolution in the primordial asteroid belt requires that certain assumptions be made about the excitation of asteroid belt bodies at that time. One also has to consider to importance of external populations that were in position to strike main belt asteroids as well. The best one can do at this time is to use dynamical models to set limits on the nature of these populations (see chapter by Morbidelli et al.).

The good news is that the main belt population has potentially been dynamically excited for most of its lifetime, with bodies filling most zones of stability between 2-3.2 AU, at least up to certain modest inclinations. If true, the primordial values of P_i and $V_{\rm imp}$ for main belt objects striking one another has stayed approximately the same since close to the planetesimal formation epoch. If the mass deficit discussed in Sec. 1 was real, collisional evolution over most of the main belt's history has been dominated by asteroids beating up on themselves.

The bad news, at least from a modeling perspective, is trying to figure out how to treat the mass deficit issue. If the primordial main belt once had considerably more mass, the dynamical processes that forced it out of the main belt zone also created numerous high eccentricity and inclination bodies that would continue to strike the surviving main belt asteroids for several to tens of Myr. A related issue is that the primordial main belt has likely been struck by sizable but short-lived populations on planet-crossing orbits, such as leftover planetesimals (Bottke et al. 2006), ejecta from giant impacts in the terrestrial planet region (Bottke et al. 2014), comets dispersed from the primordial disk during giant planet migration (Brož et al. 2013), and objects impacted in the inner solar system via giant planet migration (Walsh et al. 2011). Most of these dramatic events are thought to take place between the first few My and ~ 500 My of Solar System history.

Regardless, using dynamical models of these processes, it is possible to compute P_i and $V_{\rm imp}$ between the impacting bodies and the main belt targets. From there, it is a matter of estimating the initial sizes of the populations, how fast they disperse, and how the populations undergo collisional evolution amongst themselves.

2.2 Asteroid Disruption Scaling Laws

A second key issue to modeling asteroid collisional evolution concerns the disruption scaling law. This is commonly refereed to as the critical impact specific energy $Q^*_{\rm D}$, the energy per unit target mass delivered by the projectile required for catastrophic disruption of the target (i.e., such that one-half the mass of the target body escapes). A considerable amount has been written about the value of $Q^*_{\rm D}$ (e.g., Benz and Asphaug 1999; Holsapple et al. 2002; Asphaug et al. 2002; Davis et al. 2002), and the latest on the computation of this value can be found in the chapter by Jutzi et al. For these reasons, we only briefly review the main issues here.

Using $Q^*_{\rm D}$, the diameter of a projectile $d_{\rm disrupt}$ capable

of disrupting a target asteroid ($D_{\rm target}$) can be defined as:

$$d_{\rm disrupt} = (2Q^*_{\rm D}/V^2_{\rm imp})^{1/3} D_{\rm target} \quad (2)$$

where $V_{\rm imp}$ is the impact velocity. We assume here that the target and projectile have the same bulk density, though that is by no means assured. Small asteroids are considered part of the "strength-scaling" regime, where the fragmentation of the target body is governed by its tensile strength. Large asteroids, on the other hand, are considered part of the "gravity-scaling" regime, where fragmentation is controlled by the self-gravity of the target.

Values for $Q^*_{\rm D}$ have been estimated using both laboratory experiments (e.g., see recent review by Holsapple et al. 2002) and numerical hydrocode experiments (e.g., see recent review by Asphaug et al. 2002 and the chapter by Jutzi et al.). As summarized by Asphaug et al. (2002), Holsapple et al. (2002), and Davis et al. (2002), laboratory experiments and hydrocode modeling work suggests the transition between the regimes occurs in the range $100 < D < 200$ m.

Benz and Asphaug (1999) found that the the mass of the largest remnant after a collision can be fitted as a function of Q/Q^*_D, where the kinetic energy of the projectile per unit mass of the target is denoted by Q:

$$M_{LR} = \left[-\frac{1}{2}\left(\frac{Q}{Q^*_D} - 1\right) + \frac{1}{2}\right] M_T \quad (3)$$

for $Q < Q^*_D$ and

$$M_{LR} = \left[-0.35\left(\frac{Q}{Q^*_D} - 1\right) + \frac{1}{2}\right] M_T \quad (4)$$

for $Q > Q^*_D$, where M_T is the target mass. Whenever $M_{\rm LR}$ in Eq. (3) turns out to be negative, we assume that the target is fully pulverized, such that all of its mass is lost below some minimal mass threshold.

2.3 Asteroid Fragmentation

One the most difficult issues to deal with in any collisional evolution model is the treatment of the fragment size-frequency distribution (SFD) created when two bodies slam into one another. Given the wide range of parameters that could be involved in any collision, such as impact velocity, projectile and target sizes, impact angle, projectile and target properties, etc., it is a somewhat quixotic task to try to generate a "one size fits all" recipe capable of reproducing the outcomes of all meaningful cratering and catastrophic disruption events that could have ever taken place in the asteroid belt.

Beyond this, it is important to recognize that our asteroid belt has been subject to an enormous number of stochastic events and that information about the fragments produced by ancient collisions has been lost by subsequent collisional and dynamical processes. The upshot is that the initial conditions for ancient family-forming events or even large cratering events (see chapter by Nesvorný) may never be precisely known. A good example of this is the impact event

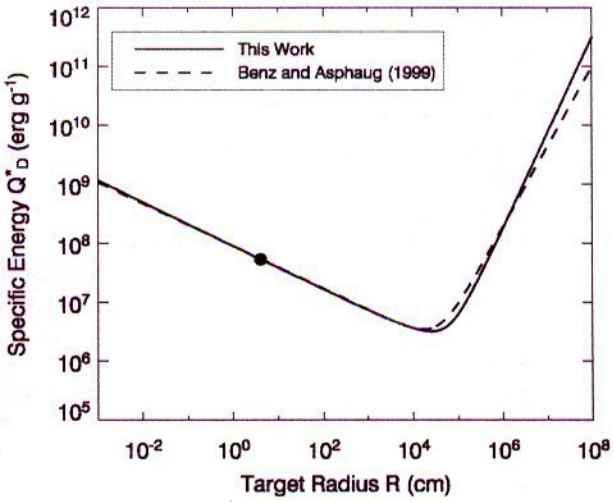

Fig. 1.— The critical impact specific energy $Q^*_{\rm D}$ defined by Benz and Asphaug (1999). This function is the energy per unit target mass delivered by the projectile that is required for catastrophic disruption of the target, such that one-half the mass of the target body escapes. The dashed line is the function derived by Bottke et al. (2005) for their modeling results. Both functions pass through the normalization point ($Q^*_{\rm D}$, D) set to (1.5×10^7 erg g^{-1}, 8 cm). This value was determined using laboratory impact experiments (e.g., Durda et al. 1998).

that created the partially buried and largely destroyed 400 km Veneneia basin on (4) Vesta.

Recognizing this fundamental limitation, a realistic modeler does the best they can with what they have. This means running their models against the constraints that do exist, though with some wariness about the limitations faced. This also means running simulations over numerous trials in an attempt to characterize how outcomes may have been affected by chance events, such as the disruption of large breakup of an asteroid at a strategic time or place that did not happen in our asteroid belt.

To this end, modern collisional evolution models have folded into their work outcomes of numerical smoothed particle hydrocode (SPH) simulations that account for at least some of the parameters described above. For example, Morbidelli et al. (2009) calculated an algorithm that reproduced the fragment size distribution of the SPH results determined by Durda et al. (2004; 2007), who conducted a large number of collision simulations of projectiles of various masses and velocities striking 100 km diameter asteroids. They found that most catastrophic collisions produce fragment SFDs that have a continuous, steep power-law size distribution starting from a single large fragment that is well separated in size from that of the largest remnant of the target. The mass of the largest fragment and the slope of the power-law SFD in each of the experiments from Durda et al. (2007) was described as a function of the ratio Q/Q^*_D that characterized each experiment.

similar relations were derived for rubble-pile targets with macro porosity (Benavidez et al. 2012), see Cibulková et al. (2014)

$$M_{LF} = 8 \times 10^{-3} \left[\frac{Q}{Q^*_D} \exp^{-\left(\frac{Q}{4Q^*_D}\right)^2} \right] (M(i) + M(j)) \quad (5)$$

for the mass of the largest fragment and

$$q = -10 + 7 \left(\frac{Q}{Q^*_D} \right)^{0.4} \exp^{-\frac{Q}{7Q^*_D}} \quad (6)$$

for the slope of the cumulative power-law size distribution of the fragments. These equations represent empirical fits to the numerical hydrocode data.

For fragment SFDs with very steep slopes, Eqs. (5) and (6) can easily exceed the mass of the projectile and target, which is non-physical. To avoid this problem, it is reasonable to assume that the fragment SFDs bend to shallower slopes at small sizes, though the precise diameter where this takes place is unknown and beyond the resolution limit of existing SPH impact simulations.

It can be shown that the derived fragment SFDs from these simulations reproduce many attributes of observed asteroid families (Durda et al. 2007). With that said, however, collisional outcomes and fragment SFDs are strongly affected by gravitational forces, with the outcomes of impacts onto 400 km targets differing from those of 100 km in terms of Q/Q^*_D [Paula's new paper; REF]. The same is probably true for smaller targets as well. An enormous advance in will therefore come from collisional evolution codes that have fragment SFDs well suited to any possible collisional outcome.

2.4 Dynamical Depletion of Main Belt Asteroids by the Yarkovsky Effect

As described in the chapter by Vokrouhlický et al., $D < 40$ km asteroids in the main belt slowly drift inward toward or outward away from the Sun in semimajor axis by Yarkovsky thermal forces. ~~In some cases~~, this allows bodies to reach resonances with the planets that drive them onto planet-crossing orbits, thereby allowing them to escape the main belt region altogether. Additional mobility is provided by encounters with big asteroids like Ceres and Vesta, though the net effect of this mechanism is fairly modest [REF].

The Yarkovsky effect, working on concert with resonances, therefore constitute a "sink" for small main belt asteroids. Their depletion should feed back into the collisional evolution of the main belt itself (i.e., fewer smaller bodies means fewer cratering and disruption events among larger bodies). It also means that the near-Earth object population can be considered an extension of the main belt population, such that its SFD can be used to constrain the nature of collisional and dynamical evolution within the main belt.

Quantifying the small body populations lost over time via the Yarkovsky effect and resonances is a challenging task. Consider the following:

- Every major main belt resonance has a different character in its ability to produce long-lived NEOs (e.g., Gladman et al. 1997; Bottke et al. 2006)
- The flux of asteroids reaching dynamical resonances may change over time as a consequence of asteroid family-forming events. Large asteroid families can produce enormous numbers of fragments, while smaller ones that disrupt in strategic locations next to key "escape hatches" may also influence the planet-crossing population for some interval.
- The dynamical evolution of $D < 1$ km asteroids is poorly constrained because these bodies are below the observational detection limit of most surveys. Moreover, these bodies are also the most susceptible to YORP thermal torques that can strongly affect their drift direction and evolution (see next section).

So far, no one has yet attempted to model all of these factors and include them into an algorithm suitable for insertion into a collisional evolution code. It is a necessary but daunting task to do this correctly, given the current state of our knowledge of how the Yarkovsky/YORP effects modify the orbits, sizes, and shapes of small asteroids.

Instead, the best that has been done to date has been to generate loss rates for the asteroid belt that produce a steady state population of NEOs (Bottke et al. 2005) (Fig. X). This approximation can provide one with several interesting insights; for example, not including the Yarkovsky/resonance "sink" can have a substantial effect on the collisional evolution of the main belt, with more projectile left behind to disrupt larger main belt asteroids.

2.5 Asteroid Disruption By YORP Torques

The Yarkovsky-O'Keefe-Radzievskii-Paddack (YORP) effect is a thermal torque that, complemented by a torque produced by scattered sunlight, can modify the rotation rates and obliquities of small asteroids (see chapter by Vokrouhlický et al.). Asteroid obliquities ~~and spin rates~~ significantly affect how fast an asteroid drifts across the main belt, and therefore how quickly it reaches a resonance that can take it out of the main belt. YORP can also spin asteroids up or down. If the body has substantial unconsolidated material, or is a rubble pile, it must reconfigure itself to adjust to the new rotational angular momentum budget. In some cases, this can cause the body to shed mass, potentially creating a binary or an asteroid pair (see chapter by Vokrouhlický et al. and REF).

The issue is whether YORP spin up is so efficient at causing small asteroids to shed mass that this mechanism dominates the production and elimination of bodies via collisional evolution in the same size range. This prospect is exciting, and it should be thoroughly investigated with a wide range of models. Initial trials suggest YORP mass shedding effects may very well dominate the behavior of $0.1 \lesssim D \lesssim 1$ km bodies [Jacobson et al. paper; REF]. With

that said, however, the model in question has not yet been subjected to the constraints discussed in Sec. 3.

We caution that our understanding of how YORP is affected by small topographic changes in an asteroid is in its infancy. For example, Statler (2009) used numerical simulations to show that modest changes in an asteroid's shape, such as the formation of a small crater or even the movement of a boulder from one place to another, could modify the YORP torques and therefore could translate into meaningful changes to the magnitude and sign of the change in rotation rate. This could prevent small asteroids from undergoing mass shedding as often as expected in current models (Cotto-Figueroa 2013; Bottke et al. 2014). This is a very important area for future research.

3. CONSTRAINTS ON COLLISIONAL EVOLUTION MODELS

Given the large number of "knobs" that exist in collisional evolution models, and the fact that these codes may provide the user with non-unique solutions, it is imperative to test the results of these models against as many constraints as possible. Given the breadth of predictions for such codes, this means accounting for how individual asteroids, asteroid families, and different asteroid populations have taken on their current status. With sufficient constraints, bad parameter choices can be eliminated from contention. On the other hand, it is important that one recognize that our understanding of main belt evolution is limited, and the inclusion of faulty constraints into a code can also produce inaccurate results and poor predictions. Accordingly, most constraints should be treated with some caution, with the modeler and interpreter cognizant that both data and interpretation can and often do change with time.

With these caveats, we present a list of many of the constraints that should be considered when modeling the evolution of the main belt.

3.1 Wavy Main Belt Size Frequency Distribution

The most fundamental constraint on collision evolution models comes from the main belt size frequency distribution (SFD). Key advances that can help one obtain better estimates of this SFD are provided by pencil beam studies of the population [Gladman et al. REF], the addition of asteroids colors from the Sloan Digital Sky Survey (SDSS) [REF], and new infrared data of many main belt asteroids provided by [Mainzer et al. REF; AKARI]. The inclusion of all of these data sets into a single debiased SFD, however, has yet to be attempted, and it is beyond the scope of this chapter.

In this chapter, it is sufficient for our purposes to derive an approximate main belt SFD using the absolute magnitude H distribution provided by Jedicke et al. (2002), who combined results from the Sloan Digital Sky Survey (SDSS) for $H > 12$ (Ivezić et al. 2001) with the set of known main belt asteroids with $H < 12$. To transform the H distribution into a size distribution, we assumed the relationship between asteroid diameter D, absolute magnitude H, and visual geometric albedo p_v (e.g., Fowler and Chillemi 1992) was

$$D = \frac{1329}{\sqrt{p_v}} 10^{-H/5}. \quad (7)$$

Here we also follow the approximations made by Bottke et al. (2005), who set p_v to 0.092 and include the observed asteroids for $D > 300$ km using the diameters cited in Farinella and Davis (1992). The population is shown in Fig. X. 2

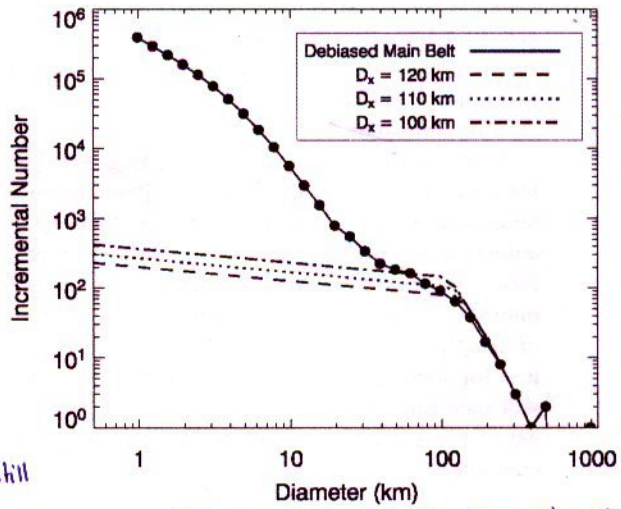

Fig. 2.— Estimates of the initial shape (dashed lines) and observed shape (solid line) of the main belt size distribution. The real primordial population was larger than this, with most of the mass eliminated by dynamical processes. The primordial shape for $D > 200$ km asteroids was chosen to be close to those in the observed main belt, assuming that a limited number of these objects ever disrupt. For $D < 200$ km objects, the slope followed an incremental power law index of -4.5 until reaching the transition point D_x. Bottke et al. (2005) tested D_x between 80 and 120 km and found that 110-120 produced the best matches to constraints. For $D < D_x$, the size distribution was given a shallow slope (-1.2). Modest changes to this value do not affect our results.

We find that the main belt SFD is wavy, with "bumps" near $D \sim 3$ km and one near $D \sim 100$ km. The reason for these bumps will be discussed in Sec. 4.

3.2 Asteroid Families

Asteroid families provide another powerful way to constrain asteroid collisional models. As discussed in the chapter by Nesvorný et al., these remnants of cratering and catastophic disruption events are identified in the main belt by their clustered values of proper semimajor axes a_p, eccentricities e_p and inclinations i_p. The problem is using them to test our model runs are that estimates of ancient family

small families

systematically ?

ages can be imprecise (see chapter by Vokrouhlický et al.) and they can also be eliminated over time by collisional and dynamical processes.

For this reason, Bottke et al. (2005) argued that one should look for complete sets of families where the parent body was large enough that their fragments could not be erased over 4 Gy of evolution. Using results discussed in Durda et al. (2007) (see also Cibulková et al. 2013), there are approximately 20 observed families created by catastrophic disruptions of parent bodies with sizes $D_{\rm PB} > \sim 100$ km, where the ratio of the largest fragment's mass to the parent body mass is $M_{\rm LR}/M_{\rm PB} < 0.5$. Bottke et al. (2005) also used the distribution of the family sizes to compare model to data. Specifically, they used the results discussed in Durda et al. (2007) to argue that the number of families formed over the last 3.5 Gy by catastrophic breakups of parent bodies whose sizes were within incremental bins centered on diameters $D =$ 123.5, 155.5, 195.7, 246.4, 310.2, and 390.5 km were 5, 5, 5, 1, 1, 1, respectively. New ~~results discussed~~ in the chapter by Nesvorný et al. can be used to update these values. (Fig. 3)

family identifications

The issue is that a superior collisional model must account for all types of collisions, even relatively small cratering events. For the purpose of comparison with observations, one has to carefully select synthetic events which would still be observable. Even though this number ($N_{\rm fam} \sim 20$) appears well defined above, it is difficult to assess its uncertainty for the following reasons:

- Determining the size of the parent of an asteroid family depends on the existing fragment distribution, which has experienced collisional and dynamical evolution, and the nature of the precise breakup involved, which may be uncertain. The existence of interlopers within the family can also be hard to exclude.

observed

- ~~There are differences between synthetic and semi-analytic proper elements~~ which may again affect the membership in a family;

We now believe synthetic elements...

individual

- There are overlapping families that are difficult to separate unambiguously (e.g. in the Nysa/Polana region);

- The method used for the parent-body size determination in Durda et al. (2007) may exhibit some systematic issues since it involves a number of assumptions.

← Taken together, the uncertainty of $N_{\rm fam}$ is at least the order of a few, if not more.

The distribution of the dynamical ages of families, as derived using the methods in the chapter by ~~Vokrouhlicky et al.~~, also provides another metric to estimate family completeness (Fig. X). We find that there are approximately the same number of young ($t_{\rm age} < 2$ Gyr) and old (> 2 Gyr) families produced by the catastrophic disruptions of $D_{\rm PB} > 100$ km bodies. This would suggest that we are indeed able

Nesvorný et al. 4

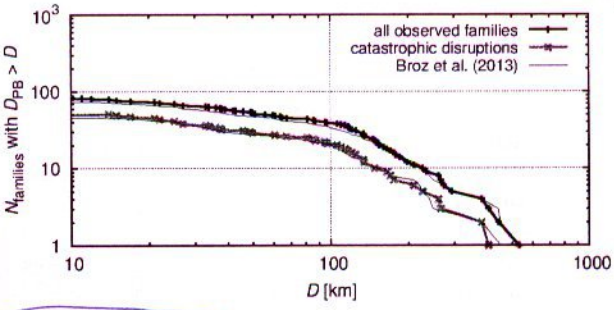

Fig. 3.— FILL THIS IN. already sent

to recognize ancient disruption events, with families found over the entire span of 4 Gy.

~~On the other hand~~, the distribution of the ~~parent~~ body sizes shown in Fig. X ~~indicates that~~ most $D > 200$ km breakups ~~took place~~ between 2-4 Gyr ago, ~~with none in the last 2~~ Gy. We find this odd, and it leaves us with the impression that something important has been missed. It could be as simple as inaccurate parent body sizes and ages, both which are difficult to calculate for ancient families. More work on all these issues are needed.

this might be only small-number statistics!

One way to account for the unusual distribution of families in Fig. X is to assume that some small families are are actually remnants, or "ghosts", of much larger older families. An possible example might be the cluster of asteroids near asteroid (918) Itha. It exhibits a very shallow SFD, which could be a possible outcome of comminution and dynamical evolution by the size-dependent Yarkovsky effect. An excellent place to look for ghost families would be the narrow portion of the main belt with semimajor axis a_p between 2.835-2.955 AU. This pristine zone, which is bounded by the 5:2 and 7:3 mean-motion resonances with Jupiter, has a limited background population of small asteroids. We postulate it could resemble what the primordial main belt looked like prior to the creation of many big families.

(Brož et al. 2013)

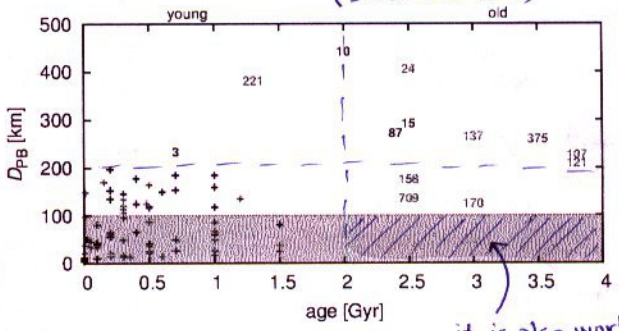

it is also worth to mention this empty region

Fig. 4.— FILL THIS IN. ditto

basins on

3.3 Impact ~~Record of~~ (4) Vesta

(4) Vesta is one of the most singular asteroids in the main belt. Not only is it among the three largest asteroids, with

there is a problem with $D_{\rm PB}$ in between 100 – 200 km! ← clearly uneven distribution in $t_{\rm age}$

↑ focus on this issue!

a diameter of 525 km [REF], but it is also has a largely intact basaltic crust that was emplaced shortly after it differentiated some 2-3 My after CAIs. We do not consider the impact record on Vesta prior to this time, though there may be interesting evidence for what happened to this world from its abundance of highly siderophile elements [REF] and composition [REF]. Decades of ground-based observations, combined with the in situ observations of Vesta by the Dawn spacecraft, have shown that the spectral signatures found in Vesta's crust are a good match to the eucrites, howardites, and diogenite meteorite classes [REF].

Vesta also has two enormous basins that dominate its southern hemisphere: Rheasilvia, a 505 km diameter crater with an estimated crater retention age of 1 Gyr, and Veneneia, a 395 km crater with a crater retention age of > 2 Gyr. Rheasilvia, being younger, overlaps with and has largely obscured Veneneia. The formation of each basin is also thought to have produced a set of fracture-like troughs, or graben, near Vesta's equator [REF]. Studies of each trough group show they form planes that are orthogonal to the basin centers. Recent simulations of the formation of the Venenia and Rhealsilvia basins using numerical hydrocodes suggest they were created by the impact of 60-70 km diameter projectiles hitting Vesta near 5 km/s (Jutzi et al. 2013). These same events likely produced the majority of the observed Vesta family, a spread out swarm of $D < 10$ km V-type asteroids in the inner main belt with inclinations similar to Vesta itself (see chapter by Scott et al.).

Vesta shows no obvious signs that basins similar in size were erased or buried once its basaltic crust was emplaced; nothing notable is detected in Vesta's topography, and there are no unaccounted for sets of troughs that could be linked with a missing or erased basin. This means Vesta is probably complete in Rheasilvia- or Veneneia-sized basins. This constrains both the size of many primordial populations as well as how long they could have lasted on Vesta-crossing orbits (e.g., main belt asteroids, leftovers planetesimals from terrestrial and giant planet formation, the putative late heavy bombardment population, Jupiter-family comets, etc.).

As a worked example, consider that if we use the main belt asteroid population described in Bottke et al. (1994), where there are 682 main belt asteroids with $D > 50$ km (see Sec. 2), we find that probability that Vesta has 0, 1, 2, or 3+ Rheasilvia/Veneneia formation events over the last 4 Gy is 50%, 35%, 12%, and 3%, respectively. If Rheasilvia and Veneneia are both < 2 Gy old, however, these values change to 70%, 25%, 4%, and 0.5%, respectively. The 4% probability for the observed situation is surprisingly small, and it suggests two possibilities: Veneneia's crater retention age was strongly affected by the Rheasilvia formation event, and the age is suspect (Marchi et al. 2012), or the basins on Vesta's surface beat the odds. Note that testing modestly smaller projectiles to make the basins, such as $D > 35$ km asteroids (Asphaug et al. 1996), only increases the probabilities above by a factor of 2 or so.

These calculations get even more interesting if we assume the main belt population was larger in its early history, and/or that it was hit by objects from outside the main belt (see chapter by Morbidelli et al.). Bottke et al. (2005) argued the main belt experienced the equivalent of 7.5-9.5 Gyr of collisional evolution over the last 4.56 Gy (i.e., roughly translated as the number of impacts Vesta would get if it resided in the current main belt population for this time; see Sec. 4). For simplicity, we round this value to 10 Gyr, which makes the probability of getting 0, 1, 2, or 3+ basins at any time in Vesta's history 17%, 30%, 27%, and 20%, respectively. This would place Rheasilvia/Veneneia near the center of the probability distribution.

If Rheasilvia/Veneneia formed < 2 Gyr ago, however, we not only have to explain their existence, but also the absence of ancient basins; large primordial populations are more likely to create ancient basins than young ones. The probability of these events taking place is only $\sim 1\%$.

Therefore, from a purely statistical point of view, one could argue that the main belt was probably more massive in the past, and that Veneneia's ~ 2 Gyr old crater retention age is not its formation age. An older age for Veneneia would also allow it to be the source for numerous Vesta family members with low inclinations, which need billions of years to reach these orbits via Yarkovsky drift and resonances (Nesvorny et al. XXXX). Further work will be needed to see if the "facts on the ground" confirm or reject these predictions.

3.4 Near-Earth Asteroids, Asteroid Craters, and Lunar Craters

The size frequency distribution (SFD) of main belt asteroids between ~ 10 m and a multi- km can potentially be directly constrained over long intervals by the crater SFDs found on asteroids. Moreover, because the main belt produces planet-crossing asteroids via the combined Yarkovsky/YORP effects, near-Earth asteroids (NEAs), as well as craters and impact byproducts found on the Moon and terrestrial planets, can also be used to indirectly glean insights into the evolution of the main belt over a wider size range of impactors.

The key issue for all these data is interpretation; the ages and/or SFDs of/on cratered terrains are often uncertain or complicated, and short-term changes in the flux or shape of impacting SFDs can be hard to decipher amid the integrated histories of cratered surfaces.

For this reason, a full discussion of all of cratering issues is beyond the scope of this section. Instead, we provide here a brief summary of how crater and NEA data [REF] can be used as constraints, provided appropriate caution is employed by the reader.

The crater histories of the asteroids visited by spacecraft are reviewed in the chapter by Marchi et al. They show that the small crater populations that do the best job of showing off the main belt production population are found on Gaspra and Vesta. The cumulative crater SFD found on or near Vesta's Rheasilvia basin show, from large to small craters,

a wavy shape: a steep slope up to an inflection point at 20-30 km, a shallow slope to an inflection point of 4 km, an even shallower slope to 0.8 km, and a steep slope to 0.1 km, where the resolution limit is reached. Note that the craters on the Marcia crater on Vesta, and on the fresh terrains on Gaspra's surface, have the same slope as that found on Rheasilvia for < 0.8 km craters. If we assume the scaling relationship between asteroids and craters is a factor of 10 (Bottke and Chapman 2006; Marchi et al. 2013), these values yield a wavy asteroid SFD with inflection points at 2-3 km, 0.4 km, and 0.08 km.

We can perform a similar analysis for the crater populations found on the Copernican and Eratosthenian terrains on the Moon. These terrains are thought to be younger than 3.2 Ga, the representative ages returned by Apollo 12 samples. For lunar craters, the broad shapes are the same as that above, with inflection points at 65-70 km, a possible one at 14 km, 2-3 km, and 0.3 km. Using crater scaling law relationships from Melosh (1989), these values roughly correspond to 2-3 km, 0.08 km, 0.04 km, and 0.004 km.

Not only does the asteroid and lunar crater data presented above agree with reasonable accuracy, but the approximate shape of the SFDs and location of the inflection points appear to be a good match to what is know about the present-day NEO population [REF]. Collectively, these results imply the shape of the main belt SFD for asteroid sizes smaller than 5-10 km has probably been in steady state for billions of years.

In terms of absolute numbers, estimates of the $D <$ 1 km craters on the Moon on specific Copernican and Eratosthenian-era terrains suggest the impact flux of very small impactors has been constant, with in a factor of 2 or so, for the last 3 Gyr. This suggests the main belt SFD for asteroids smaller than 100 m has probably been constant over the same time period. For larger lunar craters, and larger main belt asteroids, the record and interpretation are more complicated, with asteroid family-forming events potentially affecting what we see for certain intervals. Given the present state of knowledge, however, it is fair to say that deviations from a steady state are probably limited at best.

3.5 Main Belt Binaries Formed by Impacts

The population of certain types of asteroid binaries may also constrain the collisional evolution of the main belt. Using numerical hydrocode simulations to model asteroid impacts on $D = 100$ km target bodies, Durda et al. (2004) found that large-scale cratering events can create fragments whose trajectories can be changed by particle-particle interactions and by the reaccretion of material onto the remnant target body. Under the right circumstances, impact debris can enter into orbit around the remnant target body, which is a gravitationally reaccreted rubble pile, to form a SMAshed Target Satellite (SMATS).

We expect SMATS to be ~~largely~~ isolated in space; while their formation events produce asteroid families dominated by small fragments, most of these bodies are readily removed or dispersed by collisional and dynamical evolution. Detection limits of present ground-based adaptive optics searches also limits the discovery of SMATS to primary-to-secondary diameter ratios smaller than 25 (e.g., Merline et al., 2002a). For that reason, we focus here on SMATS with ~~primary-to-secondary~~ diameter ratios smaller than 25, which are presumably close to complete. In a survey of 300 large main belt asteroids, Merline et al. (2001; 2002a) reported that ~~4~~ $D > 140$ km bodies that had relatively large satellites (i.e., $D > 10$ km) that were also not in substantial asteroid families: (22) Kalliope, (45) Eugenia, (87) Sylvia, and (762) Pulcova.

Additions since that time to the SMATS record could include (216) Kleopatra and (283) Emma, whose primaries have diameters that are nearly 140 km. The secondary sizes of Eugenia and Emma, however, are very close to our primary-to-secondary diameter ratio limit, and Kleopatra appears to have an iron rather than stony composition, such that the results of Durda et al. (2004) may not be applicable. This leaves the net value somewhere in the range of 3-6. The binary (90) Antiope is excluded here because it is a likely byproduct of the Themis family-forming event; Durda et al. (2004) classifies SMATS made by catastrophic collisions in a different manner.

Using their runs, Durda et al. (2004) estimated that the expected frequency of SMATS-forming events by non-catastrophic collisions in the present-day main belt was $f = 0.9\text{-}1.7 \times 10^{?11}$ yr$^{?1}$, with the spread stemming from the collisional outcomes used in their computation. If one then assumes that the current population of $D > 140$ km bodies, $N = 94$, is similar to that from 4 Gyr ago, we would expect these production rates to yield 3-6 SMATs on average. These results are an excellent match to the 3-6 SMATs discussed above.

These results can be used to place limits on what happened during the primordial phase of the asteroid belt, depending on the planet formation evolution model invoked. For example, as described in the chapter by Morbidelli et al., the main belt potentially had an early massive phase, where numerous SMATS should have been made. A dynamical depletion event at the end of this phase would then remove most of the excess mass as well as most of the newly-formed SMATS. Effectively, this would make the remnant number of primordial SMATS the product of f, N, and the time interval that the excess population existed in the main belt. For Nice model simulations (see chapter by Morbidelli et al.), where the main belt is a few times more massive than the current population for ~ 0.5 Gyr, this would yield ~ 1 extra SMAT on average, not enough to affect the results above.

On the other hand, SMATS provide powerful constraints against scenarios where collision grinding alone removes most of the primordial mass of the main belt. This scenario is already problematic, as discussed ~~above~~ (see also Bottke et al. 2005a,b), but numerous collisions would also produce more SMATS than could be statistically justified. Similarly, some have invoked massive planetesimal populations

on terrestrial planet-crossing orbits as a way to explain various properties of the planets, the Moon, etc. (e.g., Walsh et al. 2011; Čuk et al. 2012). Many of the small bodies, however, should evolve onto asteroid belt-crossing orbits, where their collisions should create numerous SMATS. Given that observations are inconsistent with an abundance of primordial SMATS, these models can potentially be tested on this basis.

3.6 Additional Constraints

The spin vectors of asteroids in the Koronis asteroid family may also provide intriguing constraints for collisional evolution models. The Koronis family is thought to be one the asteroid belt's most ancient families, with an estimated age of 2-3 Gy [REF]. After years of painstaking observations of Koronis family members, including 21 of the 25 brightest Koronis family members, Slivan (2012) and Slivan et al. (2003; 2009) reported that nearly all of the observed 15-40 km diameter Koronis family members with prograde spins have clustered spin periods between 7.5-9.5 h and spin obliquities between 39-56°. Those with retrograde spins have obliquities larger than 140° nearly with periods either < 5 h or > 13 h. Vokrouhlický et al. (2003) demonstrated that these spin vector states were a byproduct of YORP thermal torques, (with the prograde cluster, called "Slivan states") created via an interaction between this mechanism and spin orbit resonances.

The predicted timescales for these objects to reach these spin states is several billions of years. During that time, collisions could not have strongly affected their spin periods or their obliquities; if they had, we would see at least a few bodies with more random spin vector values. Limits on this come from (243) Ida, a member of the prograde cluster with dimensions of 53.6×24.0×15.2 km; it was apparently unaffected by the formation of two ∼ 10 km diameter craters formed on its surface. *

Statistically, we would expect catastrophic disruptions events to be more rare than smaller, less energetic impact events that can modify an asteroid's spin state [REF]. In the ancient Koronis family, however, there is little evidence for the latter among the largest objects. This presents a key challenge to collisional models that assume disruption events among 20-40 km bodies are relatively common; can this outcome be reconciled with the spin states of Koronis family members?

Constraints mentioned in passing in this chapter include (i) the cosmic ray exposure ages of stony meteorites (e.g., Marti and Graf 1992; Eugster 2003; REF), (ii) the orbital distribution of fireballs (e.g., Morbidelli and Gladman 1998), and (iii) the population of V-type asteroids across the main belt (see chapter by Scott et al.).

4. INSIGHTS FROM MODELING RESULTS

The modeling work done to date on the collisional evolution of the main belt provides us with many insights into the nature of planetesimal formation, asteroid fragmentation and evolution, planet formation processes, and the bombardment history of the inner solar system. Rather than review results from all papers in the literature, we instead provide a list of some of the things we have learned from all of the modeling work.

4.1 Large Asteroids As Byproducts of Planetesimal Formation

Taking advantage of many of the constraints discussed in Sec. 3, Bottke et al. (2005) examined how one could obtain the initial shape of the main belt population. They found that the constraints in Sec. 3 pushed them toward Q_D^* functions that mimicked those derived in numerical SPH experiments of asteroid breakup events published by Benz and Asphaug (1999) (Fig. 1).

A key takeaway from the use of such disruption scaling laws is that gravitational forces make $D > 100$ km difficult to disrupt. Accordingly, the shape of the main belt for $D > 100$ km asteroids is probably primordial (Fig. 2). This insight can be used to help us better understand planetesimal formation processes (e.g., Morbidelli et al. 2009; see also chapter by Johansen et al.).

A related insight comes from tests where the power law slope of the main belt SFD between $100 < D < 200$ km, roughly -4.5, has been extended to $D < 100$ km bodies. This would create an abundance of $50 < D < 100$ km asteroids, such that the bump observed near 100 km would disappear. The problem is that these bodies are nearly as hard to disrupt as $D \approx 100$ km bodies, such that SFDs that start with these shapes have great difficulty reproducing the observed main belt SFD while also matching the constraints from Sec. 3. Bottke et al. (2005) argued that this meant the primordial main belt population with $D < 100$ km was limited, and that the bump near 100 km in the main belt SFD was primordial. A reasonable starting shape for the primordial main belt SFD for $D < 100$ km bodies would therefore be shallow (Fig. 2). This would indicate that many of the bodies seen with those sizes today are probably fragments derived from large collisions, with the ratio of fragments over primordial bodies increasing sharply as one moves away from 100 km.

This model-driven prediction, interestingly enough, is consistent with several pioneering papers from the 1950's and 1960's (Kuiper et al. 1958; Anders 1965; Hartmann and Hartmann 1968). It indicates that there is something special about the planetesimal formation process that favors the production of objects that are ∼ 100 km.

4.2 Effects of Collisional Evolution On Main Belt Size Frequency Distribution

The second bump in the main belt SFD is a byproduct of collisional evolution, and its origin given us the opportunity to revisit some classic works on this subject.

* A similar argument may come from the observed distribution of spin poles among background main belt population, which is clearly anisotropic (Hanuš et al. 2013).

Section 4.2 is too long (no title on this page...)

all of this text is old stuff... (AIII) ← you may drop it and write only 1-2 sentences as intro to O'Brien & Greenberg (2003)

The first detailed modeling of collisional cascades was by Dohnanyi (1969), who analytically modeled a population of self-similar bodies (which have the same collisional response parameters, such as strength per unit mass) and found that the steady state size distribution of such a system was a differential power law with an exponent of 3.5 ~~(actually -3.5, but the absolute value is more commonly quoted)~~. The Dohnanyi model included debris from both cratering and catastrophic disruption events, but concluded that the effect of cratering debris have a negligible effect on the size distribution. Greenberg and Nolan (1989) constructed a simple analytical model that includes only catastrophic fragmentation which also yields a steady-state power-law exponent (hereafter called the 'population index') of 3.5. This value is independent of many of the parameters describing the fragmentation process, such as the slope of the fragment distribution resulting from a catastrophic collision. Williams and Wetherill (1994) showed that even if the fragment distribution varies with impact energy (e.g., if more energetic collisions on a given body give a steeper fragment distribution as is seen in laboratory and numerical experiments), the steady-state population index will still be 3.5. This is true for any fragmentation model that is independent of the size of the target (Tanaka et al. 1996). Based on these studies, the value of 3.5 is frequently cited as the expected steady-state power-law index of a collisionally evolved population, such as the asteroid belt.

All of the above works assume that the strength ~~per unit mass~~ of the colliding bodies is independent of size. In reality, strength is strongly dependent on size, as shown by laboratory impact experiments, numerical collision models, and scaling arguments (e.g., Farinella et al. 1982; Davis et al. 1985; Housen and Holsapple 1990; Ryan 1992; Holsapple 1994; Love and Ahrens 1996; Melosh and Ryan 1997; Benz and Asphaug 1999; Housen and Holsapple 1999). They show that for bodies smaller than ~1 km in diameter, material properties cause strength to decrease with increasing size. For larger bodies, self-gravity makes it more difficult to shatter a body and disperse its fragments, leading to an increase in strength with increasing size. Hence, we obtain the classic Q_D^* function discussed above.

In general, numerical collisional evolution models have found that when strength decreases with increasing size, the power-law index of the population is greater than 3.5, and when strength increases with increasing size, it is less than than 3.5, hence the small body population where material properties dominate the strength should be steeper than the large body population where gravity dominates (e.g., Durda 1993; Davis et al. 1994; Durda and Dermott 1997; Durda et al. 1998). In addition, the transition in slope between these two different regimes leads to waves that propagate into the large end of the size distribution.

The dependence of the power-law index of the size distribution on strength parameters was explored analytically by O'Brien and Greenberg (2003), and we repeat the main results here. First consider the steady-state of a colliding population of bodies whose strength is described by a single power law. The population is described by the power law:

$$dN = BD^{-p}dD \tag{8}$$

where dN is the incremental number of bodies in the interval $(D, D+dD)$. While B should technically be negative as there are more small bodies than large bodies, it is defined to be positive here to avoid physically unrealistic result of having negative numbers of bodies in a given size interval. p is the power-law index of the population. Eq. 8 would plot as a line with a slope of $\sim p$ on a log-log plot. ~~For the classical Dohnanyi (1969) solution with size-independent strength, $p = 3.5$.~~ will be mentioned soon...

O'Brien and Greenberg (2003) considered the case where the impact strength Q_D^* is given by a power law

$$Q_D^* = Q_o D^s, \tag{9}$$

where Q_0 is a normalization constant and s is the slope of Eq. 9 on a log-log plot. They find that, in collisional equilibrium, the power-law index p in Eq. 8 is given by

$$p = \frac{7 + s/3}{2 + s/3}. \tag{10}$$

For $s = 0$, which corresponds to size-independent strength Q_D^*, of course this gives the classical Dohnanyi steady-state solution of $p = 3.5$. ~~However, if the strength Q_D^* varies with size ($s \neq 0$), p can differ significantly from the Dohnanyi equilibrium result, with $p > 3.5$ for $s < 0$ and $p < 3.5$ for $s > 0$.~~ trivial For the more realistic case where Q_D^* decreases with increasing size for small bodies and increases for larger bodies once gravity becomes important (as schematically shown in Fig. X), O'Brien and Greenberg (2003) show that the strength- and gravity-scaled portions of the size distribution have power-law indices that are only dependent on the slope of Q_D^* in the strength- and gravity-scaled regimes, respectively. The power-law index of the size distribution in the strength-scaled regime p_s has no dependence on the slope s_g of Q_D^* in the gravity-scaled regime, and vice versa; p_g is found by using s_g in Eq. 10, and p_g is found by using s_g ~~in Eq. 10~~. Since s_s is ~~generally~~ negative and s_g ~~is generally~~ positive, Eq. 10 yields a population index p_s greater than 3.5 and a ~~population index~~ p_g less than 3.5. usually

While the general slope of the size distribution in the gravity regime is unaffected by Q_D^* in the strength regime, the transition in slope of the size distribution will lead to waves that propagate through the size distribution in the gravity regime. In the derivation of ~~the population index~~ p_g ~~in the gravity-scaled regime~~, it is implicitly assumed that all asteroids were disrupted by projectiles whose numbers were described by the same power law. However, for those targets just larger than the transition diameter D_t between the strength- and gravity-scaled regimes (i.e. near the small end of the gravity-scaled regime), projectiles are mostly smaller than D_t, and hence are governed by the strength-scaled size distribution.

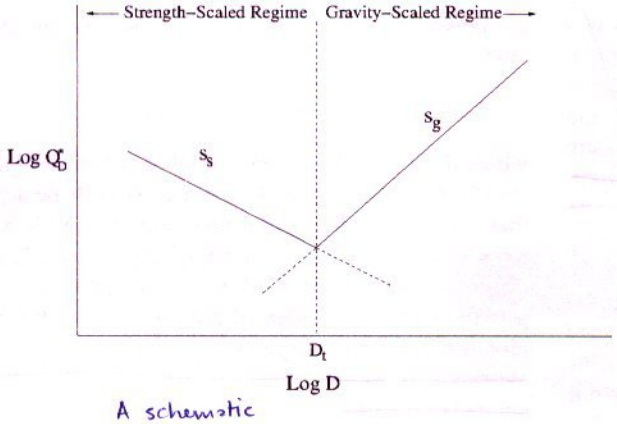

A schematic

Fig. 5.— ~~Hypothetical~~ Q^*_D law for a population with different strength properties for large and small bodies. Q^*_D consists of two different power laws with slopes s_s and s_g, joined at the transition diameter D_t. In the strength-scaled regime, material properties control the effective strength, while in the gravity-scaled regime, gravity dominates the effective strength through self-compression and gravitational reaccumulation of collisional fragments.

Consider the two steady-state power laws describing the population in the strength- and gravity-scaled regimes, joined at the transition diameter D_t as shown in Fig. 2a, and let $D_{t,dis}$ be the diameter of the body which can disrupt a body of diameter D_t. Due to the transition from the gravity-scaled regime to the strength-scaled regime below D_t, bodies of diameter $D_{t,dis}$ are more numerous than would be expected by assuming that all bodies are gravity scaled, leading to a configuration that is not in a steady state. A steady-state configuration can be achieved by 'sliding' the population in the strength-scaled regime down in number, as shown in Fig. 2b. The shift in number of bodies at D_t does not result in a simple discontinuity ~~as shown in Fig. 2b,~~ but instead causes perturbations to the size distribution in the gravity-scaled regime ($D > D_t$). The underabundance $\Delta \mathrm{Log}N(D_t)$ of bodies of diameter D_t (a 'valley') leads to an overabundance of bodies which impactors of diameter D_t are capable of destroying (a 'peak'), which in turn leads to another 'valley' and so on. This results in a wave of amplitude $|\Delta \mathrm{Log}N(D_t)|$ that propagates through the large body size distribution as shown in Fig. 2c. The average power-law index p_g of the population in the gravity-scaled regime will not be significantly changed by the initiation of this wave; the wave oscillates about a power law of slope p_g. O'Brien and Greenberg (2003) derive analytical expressions for the amplitude of the waves, as well as the approximate positions of the 'peaks' and 'valleys' in the size distribution.

DAVE - DO WE WANT TO ~~ADD SOMETHING~~ HERE ON THE REAL ~~SLOPE~~ OF ASTEROIDS IN THE ~~STRENGTH REGIME~~, AND HOW THAT YIELDS THE ~~SLOPE~~ OF Q*D?

4.3 Degree of Collisional Evolution in

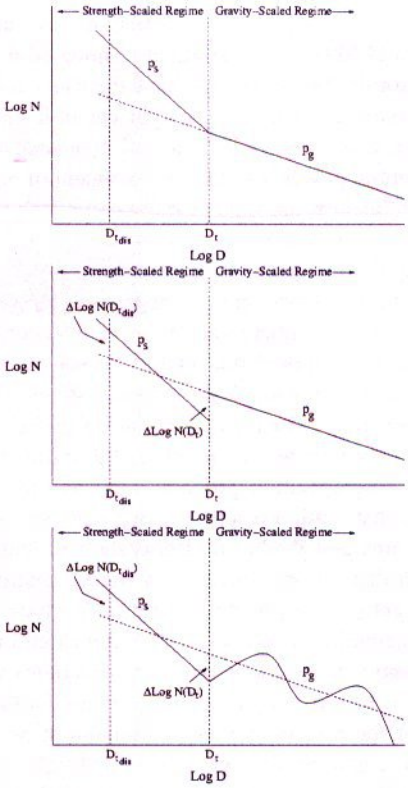

Fig. 6.— Sequence showing how waves form in the ~~population~~ as a result of a change in strength properties at D_t. (a) For a Q^*_D law such as that shown in Fig. 5, the resulting steady-state population is steeper for smaller, strength-scaled bodies (population index p_s) than for larger, gravity-scaled bodies (population index p_g). Thus, impactors capable of destroying bodies of diameter D_t are overabundant relative to what would be expected by extrapolating the gravity regime slope. This configuration is not in collisional equilibrium. (b) To counteract this, the number of bodies of diameter D_t and smaller decreases by a factor $\Delta \mathrm{Log}N(D_t)$ so that there are fewer 'targets' of diameter D_t and fewer impactors of diameter $D_{t_{dis}}$. (c) The decrease in bodies of diameter D_t leads to an overabundance of bodies which can be destroyed by impactors of diameter D_t, which in turn leads to a depletion of larger bodies and so on. Thus, a wave is formed in the large-body population.

Main Asteroid Belt

A key goal of collisional evolution models is to estimate how much comminution has actually taken place over the main belt's history. Values for this allow us to then constrain its dynamical evolution, and perhaps probe the ~~times with the main belt was conceivably more massive than it is today~~.

A useful metric to do this is as follows. First, we assume that the main belt is self-contained in terms of collisions (i.e., we ignore projectiles from leftover planetesimals, comets, etc.) and that the intrinsic collision probabilities and impact velocities of main belt asteroids hitting one

another has remaining unchanged over its history (Sec. 2). For simplicity, we can also assume the main belt's SFD has been close to its current shape throughout its history, though it may have had a larger population in the past. The degree of collisional evolution that the main belt has experienced then becomes proportional to the integral of $f \Delta T$, where f is the ratio of the main belt's SFD during a given interval ΔT over the current main belt SFD. Thus, the minimum degree of collisional evolution for a nominal main belt ($f = 1$) over its lifetime ($\Delta T = 4.5$ Gyr) would be 4.5 Gyr.

We can now include evolution scenarios. Suppose the primordial main belt immediately after planetesimal formation and its initial dynamical excitation had $f = 1000$ for 2 Myr (0.002 Gyr). At that point, we assume that most of the population was lost in the Grand Tack scenario, which reduced it to $f \sim 4$ for ~ 0.5 Gyr. Then, at ~ 4 Gyr, 75% of the bodies were lost via sweeping resonances driven by late giant planet migration, which left the surviving population close to its current state ($f = 1$) for the next ~ 4 Gyr. Collectively, the survivors experienced the rough equivalent of what $(2 + 2 + 4) = 8$ Gyr of collisional evolution would be like in the current main belt.

Using a more sophisticated model that adopted many of the constraints above, Bottke et al. (2005) found similar values; they found the main belt experienced the equivalent of 7.5-9.5 Gyr of collisional evolution in the current main belt. Their interpretation was that main belt SFD obtained its wavy shape by going through early periods where it was exposed to many more projectiles than are observed today, with most of those bodies lost to dynamical processes. Thus, the wavy main belt SFD could be considered a "fossil" produced in part by early collisional evolution in the primordial main belt.

We find it interesting that many of the main belt dynamical evolution models discussed in the chapter by Morbidelli et al. match this constraint, though we cannot argue for their uniqueness. The pseudo-age of 7.5-9.5 Gyr can also be used to explore planet formation scenarios, particularly those that create abundant projectile populations that potentially beat up on the early main belt.

{Stability of main belt and NEO populations} The models also suggest that once the shape of the main belt SFD approaches that of the current population, it will stay in steady state for billions of years. This may explain why the non-saturated crater populations on Gaspra and Vesta appear to have the same shape. Similarly, because the main belt is the main source of NEOs, we would expect the impact flux on the terrestrial planets to have been close to constant over the last ~ 3 Gy or so, with some room for the effects of asteroid family-forming events (e.g., Shoemaker and Grieve 1994).

4.4 Connections between asteroid families and meteorites

One of the most perplexing issues involving meteorite delivery concerns the fact that we currently have more than 50,000 meteorites in worldwide collisions (Grady 2000;

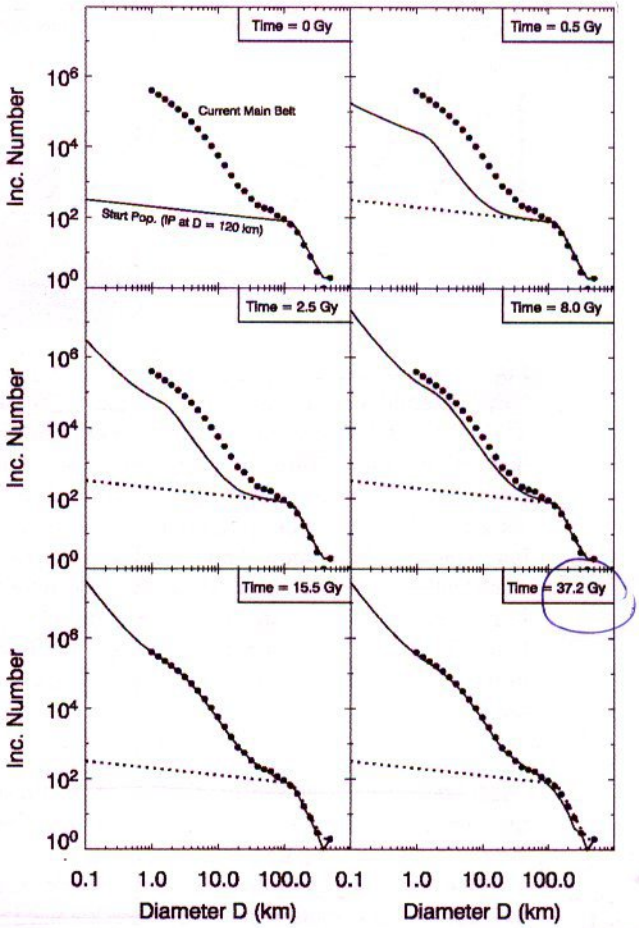

Fig. 7.— Six snapshots from a representative run where we track the collisional evolution of the main belt size distribution for a pseudo-time of 50 Gy. This run uses a starting population with $D_\# = 120$ km. The bump near $D \sim 120$ km is a leftover from accretion, while the bump at smaller sizes is driven by the transition at $D \sim 0.2$ km between strength and gravity-scaling regimes in Q^*_D. Our model main belt achieves the same approximate shape as the observed population at $t_{\rm pseudo} = 9.25$ Gy. The model closely adheres to the observed population for many Gy after this time. Eventually, comminution eliminates enough $D > 200$ km bodies that the model diverges from the observed population. From Bottke et al. (2005)

REF), yet this population could represent as few as ~ 100 different asteroid parent bodies: ~ 27 chondritic, ~ 2 primitive achondritic, ~ 6 differentiated achondritic, ~ 4 stony-iron, ~ 10 iron groups, and ~ 50 ungrouped irons (Meibom & Clark 1999; Keil 2000; 2002; Burbine *et al.* 2002). If we ignore the stony-iron, iron, and differentiated meteorites for the moment, this number is reduced to as few as ~ 30 objects. This mismatch is even more confusing given current meteorite delivery scenarios, where nearly any small main belt fragment can potentially reach a resonance capable of taking it into the terrestrial planet region via the Yarkovsky

too small

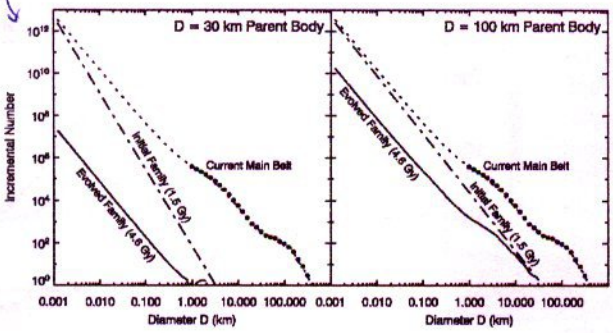

Fig. 9.— The collisional and dynamical evolution of two "toy" asteroid families produced by the disruption of a $D = 30$ and 100 km parent bodies. Both families were inserted into the collision evolution model at 1.5 Gy after solar system formation. The meteoroid population is represented by the number of bodies in the $D \sim 0.001$ km size bin. The solid lines show the families at present (4.6 Gy). The smaller family has decayed significantly more than the larger family. Note the shallow slope of the $D = 100$ km family for $0.7 \lesssim D \lesssim 5$ km. This shape mimics the that of the background main belt population over the same size range.

effect ~~(see chapter by Vokrouhlický et al.)~~. Presumably, this would give us access to samples from thousands upon thousands of distinct parent bodies.

What is missing from this picture is an understanding of how collisional evolution has shaped ~~our knowledge of~~ the asteroid belt. ~~Using the models discussed above~~, we can try to apply ~~it~~ to the issue of stony meteoroid production, evolution, and delivery to the Earth. First, let us consider when a single body undergoes a cratering or catastrophic disruption event. A fragment SFD is created that will probably include a wide range of sizes, from meteoroid-sized bodies to multi-km asteroids. Subsequent collisions onto bodies in the SFD act as a source for new meteoroids that are genetically the same as those created in the previous generation. This collisional cascade guarantees that meteoroids from this family, representing a single parent body, will be provided to the main belt population, resonances, and possibly to Earth for an extended interval. At the same time, dynamical processes and collisions onto the newly-created meteoroids act as a sink to eliminate them from the main belt. Thus, ~~after the initial collision event, the sources and sinks drive the meteoroid population toward a quasi-steady state. If the sinks dominate the sources, the meteoroid population will undergo a slow (or not so slow) decay as collisions on the FSD deplete the reservoir of larger bodies capable of replacing them. The size and nature of this reservoir, therefore, determine the decay rate of the meteoroid population.~~

An example of this is shown in Fig. X. It shows what happens when simple power law fragment SFDs produced by $D = 30$ km and 100 km parent bodies are placed in the main belt ~ 3.1 Gyr ago. For fragments derived from the 30 km body, we find that the initial meteoroid population (i.e., the population of meter-sized bodies) drops by a factor of 100 and 10^5 within 130 My and 3.1 Gy, respectively. Thus, meteoroid production by < 30 km parent bodies decay away so quickly that ancient breakup events of this size are unlikely to deliver meaningful numbers of meteoroids to Earth today. For the 100 km parent body, the decay rate is significantly slower, with the meteoroid population only dropping by a factor of 100 over 2-3 Gy. This suggests that many meteoroids reaching Earth today come from prominent asteroid families with sizable SFDs, even if those families were created billions of years ago.

Bottke et al. (2005) used these ideas to roughly estimate how many stony meteorite classes should be in our collection by combining the meteoroid decay rates taken from the kinds of evolution seen in Fig. X with their estimated production rate of asteroid families over the last ~ 4 Gy. They assumed that (i) meteoroids from all parts of the main belt have an equal chance of reaching Earth, (ii) all $D > 30$ km asteroids disrupted over the last several Gy have the capability of producing a distinct class of meteorites, and (iii) once a family's meteoroid production rate drops by a factor of 100, an arbitrary choice, it is unlikely to produce enough terrestrial meteorites to be noticed in our collection.

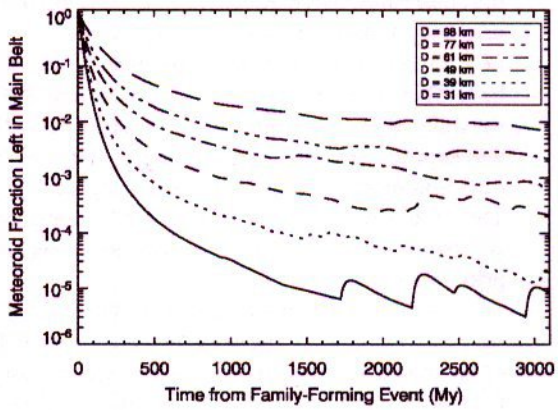

Fig. 10.— Decay rates of meteoroid populations from our "toy" asteroid families produced from parent bodies with $30 < D < 100$ km. All families were inserted in collisional model at 1.5 Gy after solar system formation. The smallest families decrease by a factor of 100 over a few 0.1 Gy while the largest take several Gy to decay by the same ~~value~~ factor.

They found that asteroid families produced by the breakup of $D \gtrsim 100$ km bodies have such slow meteoroid decay rates that most should be providing meteoroids today, regardless of their disruption time over the last 3-4 Gy. Among the smaller parent bodies ($30 < D < 100$ km), they found that, on average, the interval between disruption events across the main belt was short enough that many have disrupted over the last Gy or so, enough to provide some meteoroids as well. Overall, they found that stony meteorites could be coming from ~ 45 different parent bodies, which is fairly close to the actual value of ~ 30 parent bodies. Reasons for this value to be high include the possibility that (i) some disruption events must occur within existing

families, so no unique meteorite class would be created, and (ii) some outer main belt meteoroids may have great difficulty reaching Earth because they only have access to resonances that are orders of magnitude less efficient at delivering meteoroids to Earth than inner main belt resonance (Gladman et al. 1997; Bottke et al. 2006). These factors could easily reduce the number of sampled parent bodies in our model enough to match observations. To do this problem right, however, would require a next-generation model combining collisonal and dynamical evolution of asteroid populations.

Here ~~There~~, we conclude that most stony meteorites are byproducts of a collisional cascade, with some coming from asteroid families produced by the breakup of $D > 100$ km bodies over the last several Gy and the remainder coming from smaller, more recent breakup events among $D < 100$ km asteroids that occurred over recent times, (i.e., ~~$\ll 1$ Gy).~~ during the last few hundreds of My.

4.5 Interesting Issues ← a too general title... use LHB instead

The Nice model would also provide a large influx of comets into the inner solar system, with many potentially slamming into main belt asteroids. According to Brož et al. (2013), a massive 25 $M_\oplus$ disk of trans-Neptunian comets might contain 10^{12} $D > 1$ km comets (i.e. corresponding to the observed broken power law for the current Kuiper Belt; Fraser & Kavelaars 2008). Using numerical simulations, they estimated the collision probabilities and impact velocities for comet and main belt asteroids to be $P_i \sim 6 \times 10^{-18}$ ~ km^{-2} yr^{-1} and $V_{\rm imp} \sim 10$ km s^{-1}. Coupled with models describing the loss of asteroids during resonance sweeping, they estimated that the LHB could potentially disrupt as many as 100 parent bodies with $D_{\rm PB} > 100$ km. The fact that it is so much smaller than the observed number of 20 suggests that ~~one of the Brož et al. assumptions is wrong~~ or that additional physical mechanisms, such as comets disruptin in the inner solar system, are at work here.

of Vokrouhlický et al. (2008)

Minton & Malhotra (2010)

~ LARGER !

← rather say there are possibly many undiscovered families (or their remnants)

5. CONCLUSIONS AND OPEN PROBLEMS

FILL THIS IN

Acknowledgments. Research funds for William Bottke were provided by NASA's Solar System Evolution Research Virtual Institute program as part of the Institute for the Science of Exploration Targets (ISET). FILL THIS IN. already sent

REFERENCES

Alves, J. F., Lada, C. J., and Lada, E. A. (2001) Internal structure of a cold dark molecular cloud inferred from the extinction of background starlight. *Nature, 409*, 159-161.

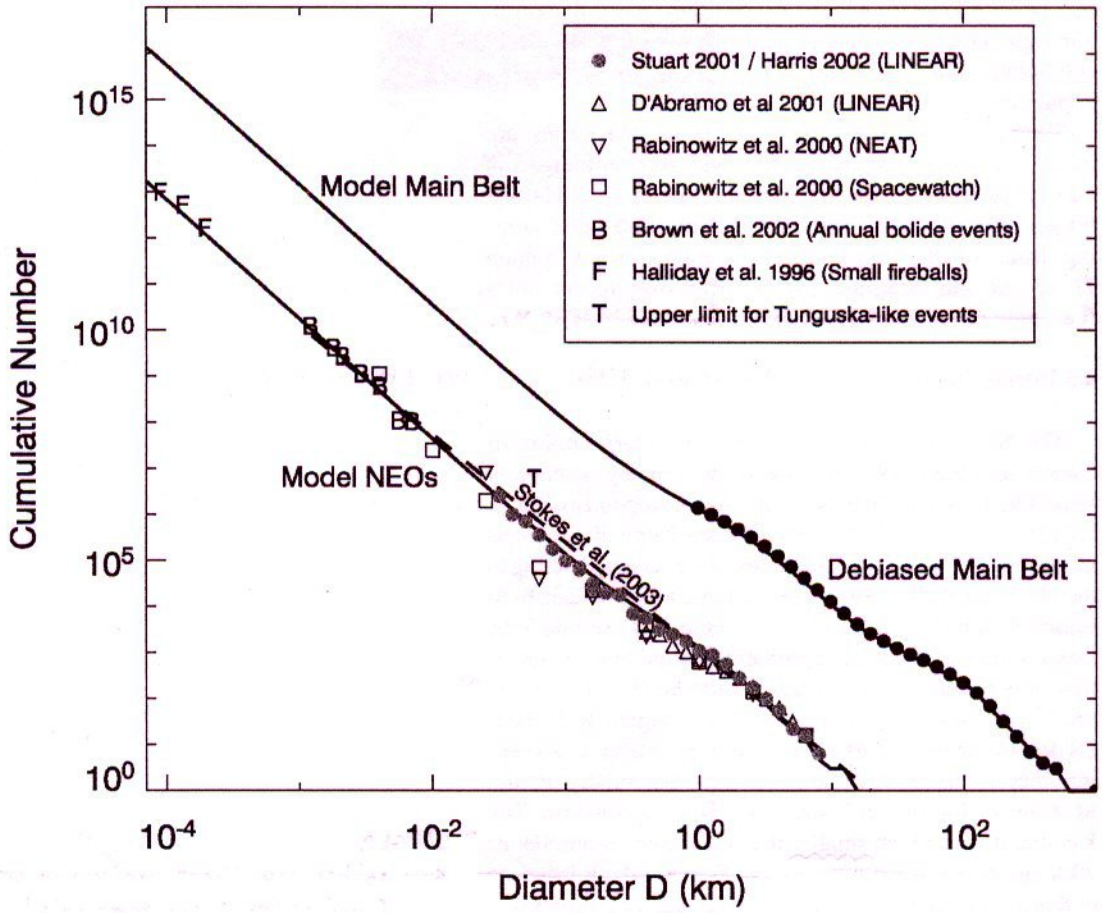

Fig. 8.— The estimated values of the present-day main belt and NEO populations according to Bottke et al. (2005) model runs (solid lines). For reference, we plot our results against an estimate of the NEO population made by Stokes et al. (2003), who assumed the $D < 1$ km size distribution was a power-law extension of the $D > 1$ km size distribution. Our model main belt population provides a good match to the observed main belt (solid black dots). Most diameter $D \lesssim 100$ km bodies are fragments (or fragments of fragments) derived from a limited number of $D \gtrsim 100$ km breakups (Bottke et al. 2005). Our NEO model population is compared to estimates derived from telescopic sur;veys (Rabinowitz et al. 2000; D'Abramo et al. 2001; Stuart 2001; Harris 2002; Stuart and Binzel 2004), satellite detections of bolide detonations in Earth's atmosphere (Brown et al. 2002), and ground-based camera observations of fireballs (Halliday et al. 1996). For reference, we also include an upper limit estimate of 50 m NEOs based on the singular airblast explosion that occurred over Tunguska, Siberia in 1908 (e.g., Morrison et al. 2002; Stokes et al. 2003). The similarity between the shapes of the main belt and NEO populations is a byproduct of Yarkovsky ~~thermal drag~~, which causes main belt asteroids with $D \lesssim 30$ km to drift into resonances that in turn deliver them to the NEO population.